Hindawi
Advances in Civil Engineering
Volume 2019, Article ID 3591629, 12 pages
https://doi.org/10.1155/2019/3591629

Research Article

Permeability Characteristic and Failure Behavior of Filled Cracked Rock in the Triaxial Seepage Experiment

Xinyu Liu ,[1,2] Zhende Zhu,[1,2] and Aihua Liu[3]

[1]*Key Laboratory of Ministry of Education for Geomechanics and Embankment Engineering, Hohai University, Nanjing 210098, China*
[2]*Jiangsu Research Center for Geotechnical Engineering, Hohai University, Nanjing 210098, China*
[3]*College of Water Conservancy and Civil Engineering, South China Agricultural University, Guangzhou 510642, China*

Correspondence should be addressed to Xinyu Liu; liuxy267@hhu.edu.cn

Received 7 May 2019; Revised 19 June 2019; Accepted 24 June 2019; Published 3 July 2019

Academic Editor: Eric Lui

Filling is commonly found in natural cracked rock mass. As the weakest part of the rock, the filling properties directly affect the rock deformation and strength, permeability, and so on and affect the safety and stability of the rock mass engineering. In this study, a single slit has been preset in sandstones and filled with different physical properties materials. Based on the laboratory triaxial seepage test, the permeability and strength characteristics of filled cracked sandstones are analyzed, and the failure modes are obtained. The main findings of this study are as follows: (1) The permeability coefficient peak value of the filled cracked rock appears before the stress peak. (2) At the same confining pressure growth rate, the peak stress growth rate of the filled cracked rock is generally higher than that of the intact rock and the strength growth rate of the cracked rock increases with the length of the fracture. The strength characteristics of the filling in the uniaxial compression tests and triaxial seepage tests are significantly affected by the hydraulic properties. (3) The strength and permeability coefficients of cracked rock filled with cement mortar are more sensitive to the change of confining pressure, while under the same condition, the ones of cracked rock filled with gypsum mortar are stable. (4) According to the failure mechanism, under the seepage stress, the secondary cracks can be divided into 3 types and the failure modes can be divided into 2 types.

1. Introduction

Under the high-pressure water, a large amount of liquid energy accumulates inside the rock mass. When the energy is concentrated to a certain extent, due to the disturbance of the excavation effect, the roof and floor of the roadway suddenly collapse to the free face, which will cause a water inrush accident. Therefore, the nonburst mines that do not generate water inrush in the shallow part will be transformed into water inrush mines with frequent water disasters after entering the deep. In the past 2007~2014 years, a total of 128 coal mine water inrush accidents have occurred in China, with a total of 702 deaths [1]. According to statistics, more than 80% of the water inrush accidents in Chinese coal mines are caused by faults [2]. The fillings in the fault zone have low tensile strength and are mostly argillaceous and carbonaceous fragments. Therefore, under the confined water, the filling material is easily softened, eroded, and hollowed out, which reduces the thickness of the aquifuge and causes favorable conditions for water inrush.

From the elastic mechanics, filling reduces the degree of stress concentration [3]. Due to the different filling patterns and filling properties, the filling cracks have different bearing capacities. Under the various complicated loads such as seepage and confining pressure, the filling cracks are easy to cause engineering instability and geological disasters, especially in the safety and stability of mines, water conservancy, bridge, mountain tunnel, and other projects. It is the core content of this paper to study the influence of filling cracks on strength, permeability, and failure of cracked sandstone in triaxial seepage experiment.

Since 1960s, French scholar Louis first proposed rock mass hydraulics as a new discipline. So far, scholars from various countries have carried out a lot of related research work. Some scholars have applied laboratory tests, NMR imaging, and discrete element method to study the permeability of cracked rock mass under the influence of structural plane roughness, trace length, and fracture surface area, verified the validity of cubic law, and proposed some correction methods for calculating permeability [4–10]. In addition, the researches show that the variation law and sensitivity of permeability under different external loads are different [11–13]. By analyzing the stress-strain-permeability curves, the relationship between rock deformation mechanism and permeability is obtained, which indicates that permeability is controlled by crack characteristics [14, 15].

At present, researchers mostly discuss factors such as the roughness, opening, and length of fractures that affect seepage characteristics. For a long time, the researches on rock filled cracks are mainly about the analysis of its shear strength, such as Toledo et al. [16], Davies et al. [17], Indraratna et al. [18], Li et al. [19], and so on.

More and more scholars have realized the influence of filling materials on the seepage characteristics of cracked rock masses and carried out relevant research work. Wealthall et al. [20] had found that when the filling is widely distributed in large fractures, the permeability of the crack shows two opposite rules. Chen and Kinzelbach [21] had proposed that the permeability of the cracked rock is affected by the fault mud. Olson et al. [22] replicated the typical low permeability of tight sandstone by filling fractures with cement and proposed a natural crack rock analysis model. Wang et al. [23] conducted a study on the seepage characteristics of cracked rock filled with silts and summarized the effect of silt particles on the permeability of cracked rock. Thörn et al. [24] used a fluid mechanics laboratory test with single cracked rock to correlate the fracture strength with fracture filling, stress history, and so on. Ono's research [25] on the Palaeogene Shimanto Belt of Kyushu in Japan demonstrated that the acid water dissolved calcite crack filling minerals to form the present groundwater flow-paths. Kavanagh and Pavier [26] used rock strength tests to investigate the effect of the rock interface on the fractures containing liquid filler in the crust. Liu et al. [27] had revealed that the influence of the stress history of fractured rock masses with sandy filler on the permeability coefficient cannot be ignored. Zhang et al. [28] had carried out the seepage test on the half-filled cracked rock and found that the seepage-stress curve of the half-filled cracked rock is more consistent with the calculated value of the cusp catastrophe theory. Chen and Zhang [29] and Chen et al. [30] used different brittle filling materials to conduct experiments and discussed the influence of the mechanical response of filling materials on the seepage characteristics. Liu et al. [31] had studied the seepage and failure characteristics of filled cracked rocks under high confining pressure.

From the scholars' study of filled cracked rock mass, it is known that the filling in the cracks makes the seepage and mechanical characteristics significantly different. Under the seepage stress, the internal structure of the rock mass changes slightly or drastically, and the filling in the crack is affected, causing its dissolution, migration, and cracking, thus affecting the permeability and strength characteristics of the cracked rock mass.

Previous studies have mainly focused on single-type fillings with low design test pressure, without considering the seepage failure characteristics of fractured rocks with fillings of different hydraulic properties in deep formation. This study is investigates the variation of permeability, strength, and fracture characteristics of filled cracked rock due to different hydrological properties of the filling under high water pressure and confining pressure. It can help us to understand the influence of the physical properties and structural characteristics of the fillings in the cracked rock mass on the seepage failure.

2. Materials and Experimental Procedure

2.1. Sample Selection and Preparation. The natural rock mass structure is complex, and the rock samples taken at the site are random and nonrepeatable. When studying the influence of cracks on the rock mass seepage damage, it is difficult to control the variables to obtain effective conclusions. At present, in the laboratory test on the permeability characteristics of the filled fractured rock mass, the cracks are usually prefabricated by cutting and splitting and then filled. There are two types of filling cracks in rock mass. One is in situ filling, which can be divided into primary filling and secondary filling. The other is artificial filling widely used in engineering and scientific research. Artificial filling materials can be divided into cemented filling, dry filling, and water-sand filling. In this study, the single crack is made in the intact sandstone by cutting. According to the common types of fillings in natural cracked rock masses recorded in Engineering Geology Site Manual, river sand, cement, and gypsum are used to fill the prefabricated cracks to complete the sample.

Sandstone, one of the most important rocks for storing hydrocarbon and water, is chosen as a rock for presetting cracks. Then materials with different hydraulic properties are poured into the fractures. The MTS815 electrohydraulic servo rock mechanics test system is used to conduct rock failure tests under the conditions of stable confining pressure and seepage pressure.

One type of filling material used in this test is gypsum mortar. Gypsum, a soluble substance commonly found in natural filling, is an air-hardening cementitious material that can only harden in air and can only maintain and develop its strength in air. It has a strong hygroscopicity, and after moisture absorption, its strength decreases significantly. Another type of filling material is cement mortar. Portland cement, a common cementitious material, is a hydraulic material. It not only hardens in the air but also hardens in water and maintains strength.

(1) Select intact sandstone (Ø50 mm × 100 mm), and use a cutting knife for presetting crack. Considering that the particle size of the later-filled quartz sand is 0.5-0.6 mm, the crack width is controlled to be about 10 times the maximum particle size of the filler, that is, about 6 mm, and the length of the crack reaches 75%, 50%, and 25% of the complete specimen, as shown in Figures 1–3.

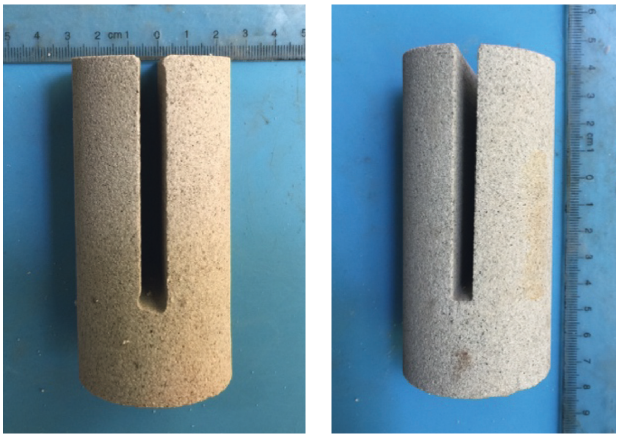

(a) (b)

Figure 1: Prefabricated crack: 6 mm width and 75% length.

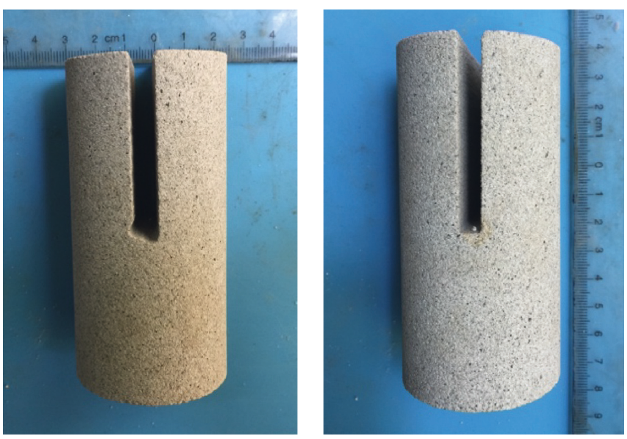

(a) (b)

Figure 2: Prefabricated crack: 6 mm width and 50% length.

(a) (b)

Figure 3: Prefabricated crack: 6 mm width and 25% length.

(2) Pour the filling slurry into the processed sandstone. The acrylic rod is used to gently vibrate during the filling process to eliminate bubbles in the filling material, ensuring the compactness and quality of the filling. One type of filling slurry is prepared according to the standard of 1 : 1.5 : 0.5 using gypsum, quartz sand, and water. Another one is formulated with white cement, quartz sand, and water in accordance with the standard of 1 : 1.5 : 0.5. The standard test pieces of the filling material are selected for the uniaxial compression test. The uniaxial compressive strength of the gypsum mortar sample is 4.27 MPa, and the one of the white cement mortar sample is 1.50 MPa. Both strengths are low, and strength of the cement mortar is lower than the gypsum mortar one and in sharp contrast to the uniaxial compressive strength of the complete sandstone (30.65 MPa).

(3) Considering that the cement mortar hardening time should be more than 14 days, the two types of filled cracked rock samples made at the same time are placed in the same indoor environment for natural curing (room temperature is about 20 degrees) for 18 days, as shown in Figure 4.

2.2. Test Principle and Result. This test is performed on the MTS815 system (as shown in Figures 5 and 6). Axial loading adopts displacement control mode, and confining pressure remains unchanged at all levels. The pore water pressure (p_2) at one end of the rock is fixed, and then the one (p_1) at the other end is lowered so that an initial osmotic pressure difference is formed at both ends. As the fluid moves through the cracks in the rock, the pore water pressure difference decreases. By measuring the decay process of the water pressure difference over a certain period of time, the permeability of the rock under this stress state can be calculated. The test method is to apply transient pulse technique to measure permeability in the laboratory. The calculation equation of the test result is written as

$$k = \frac{\mu C_w V L}{2A} \frac{\lg\left(\Delta p_i / \Delta p_f\right)}{T_f - T_i}, \tag{1}$$

where Δp_i and Δp_f are the difference in pore water pressure at the start and end of the test and T_i and T_f are the start and end time of the test.

According to the results of the in situ tests conducted by Xie et al. [32] in China, the ground stress can reach about 12.5 MPa near the depth of 500 m. When the depth reaches 750 m, the ground stress tends to 18.75 MPa, and when the depth is 1000 m, the ground stress can reach 25 MPa. And He et al. [33] had suggested that karst water pressure can be as high as 7 MPa or even higher in deep mining. Therefore, this experiment simulates the seepage failure of cracked rock when the confining pressure is 10 MPa and 20 MPa and the osmotic pressure difference is 6 MPa.

The stress-strain curve shows the process of nonlinear compaction, linear elastic process, crack development, and nonlinear failure (as shown in Figure 7). The change of the permeability-strain curve is that with the increase of strain, the permeability gradually increases and most of the maximum permeability value appears obviously earlier than the peak strength of the stress-strain curve, and then the

(a) (b)

Figure 4: Cracked rocks filled with (a) gypsum mortar and (b) cement mortar.

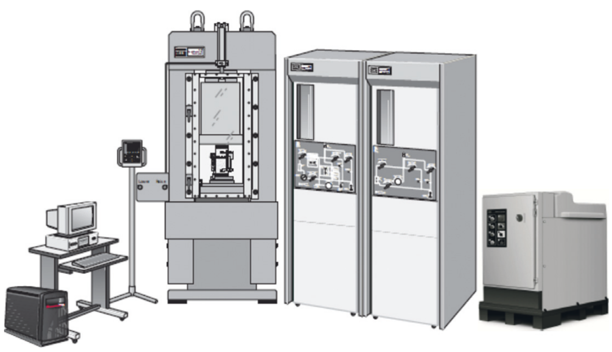

Figure 5: MTS815 system.

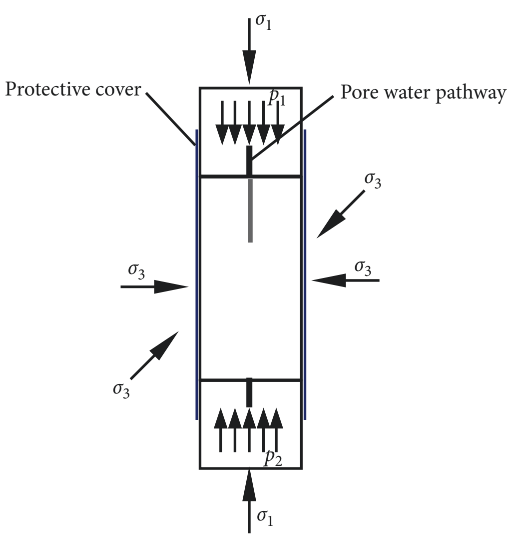

Figure 6: Rock sample in the seepage test system.

permeability enters the decline stage. The sandstone used in the test is a fine-grained brittle rock and obtains more seepage channels due to the preset filling cracks in the intact rock. After the beginning of the test, a small amount of microcracks develop and connect to form a large permeation path, which significantly increases the permeability. However, in the plastic stage, the fracture is sheared or collapsed, and the movement of the filling blocks the flowing channel so that the permeability is reduced, and the permeability peak appears before the stress peak.

According to the stress-strain-permeability coefficient curve, the data in Tables 1 and 2 are obtained. Due to the rapid softening failure of samples 1-5 (Figure 7(i)), only one set of permeability coefficients is obtained. In contrast, the seepage tests of complete sandstone are carried out and the data in Table 3 are obtained.

3. Seepage Failure

3.1. Characteristics of Permeability and Strength

(1) When the confining pressure increases, the strength of intact rock and filled cracked rock increases. According to the data in Table 4, at the same confining pressure growth rate, the peak stress growth rate of the filled cracked rock is generally higher than that of the intact rock. When the fracture fillings in the rock are the same, the strength growth rate of the cracked rock increases with the length of the fracture.

Under the same external load and fracture conditions, the strength of cracked rock filled with cement mortar is generally higher than that filled with gypsum mortar. This is contrary to their uniaxial compression test results and reflects the change in strength caused by different physical properties of fillings.

(2) Under the same load and same fractured structural plane conditions, the cracked rocks with different physical properties fillings have different sensitivities to the confining pressure.

Table 5 shows the peak strength differences for different crack length rocks under confining pressure. Due to the increase of confining pressure, the strength difference of fractured rock filled with cement mortar has dropped dramatically, which is more sensitive to confining pressure confinement effect. And the strength decline value of fractured rock filled with gypsum mortar is more stable when confining pressure changes.

(3) The permeability of the filled cracked rock decreases as the confining pressure increases. At low confining pressures, the change in permeability of filled cracked rock is generally higher than that at high confining pressure. In the three types of structural planes, the permeability change of samples with the crack length of 50% is generally larger.

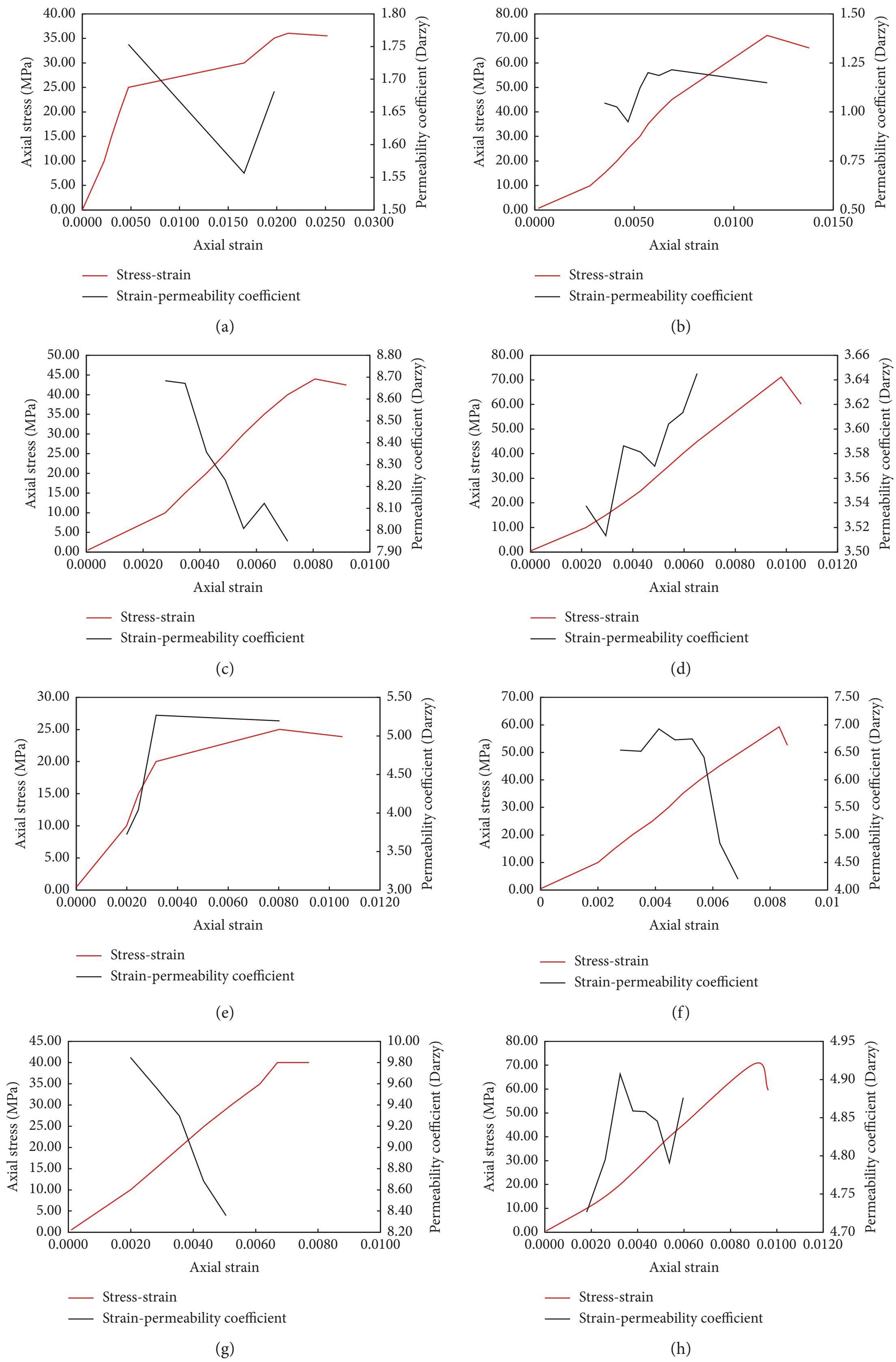

Figure 7: Continued.

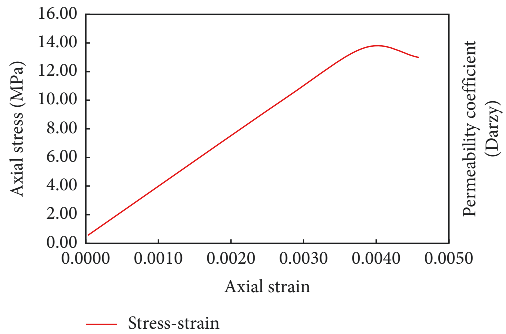

(i)

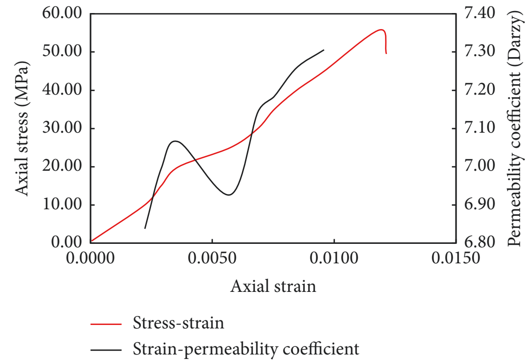

(j)

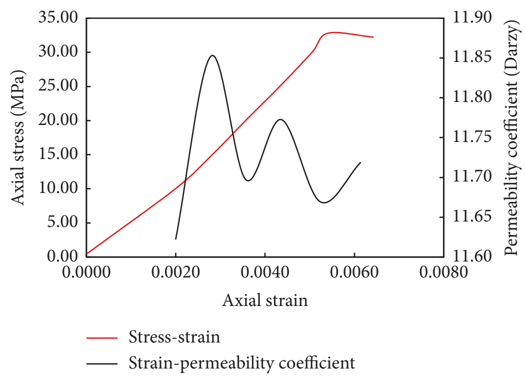

(k)

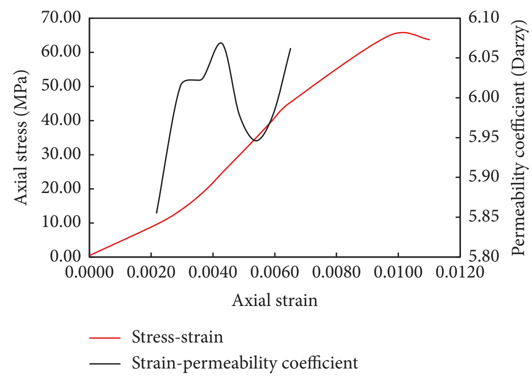

(l)

FIGURE 7: Stress-strain-permeability coefficient curve. (a) Sample 1-1: confining pressure = 10 MPa; water pressure = 6 MPa. (b) Sample 1-2: confining pressure = 20 MPa; water pressure = 6 MPa. (c) Sample 2-1: confining pressure = 10 MPa; water pressure = 6 MPa. (d) Sample 2-2: confining pressure = 20 MPa; water pressure = 6 MPa. (e) Sample 1-3: confining pressure = 10 MPa; water pressure = 6 MPa. (f) Sample 1-4: confining pressure = 20 MPa; water pressure = 6 MPa. (g) Sample 2-3: confining pressure = 10 MPa; water pressure = 6 MPa. (h) Sample 2-4: confining pressure = 20 MPa; water pressure = 6 MPa. (i) Sample 1-5: confining pressure = 10 MPa; water pressure = 6 MPa. (j) Sample 1-6: confining pressure = 20 MPa; water pressure = 6 MPa. (k) Sample 2-5: confining pressure = 10 MPa; water pressure = 6 MPa. (l) Sample 2-6: confining pressure = 20 MPa; water pressure = 6 MPa.

TABLE 1: Seepage test results of cracked sandstone filled with gypsum mortar.

Conditions and results	1-1	1-2	1-3	1-4	1-5	1-6
Sample size (mm)						
D	48.28	48.32	48.64	48.33	48.23	48.00
H	99.45	99.66	99.55	99.33	99.46	99.55
Crack length (%)	25	25	50	50	75	75
Density ρ ($g\,cm^{-3}$)	2.29	2.99	2.30	2.28	2.29	2.31
Elastic modulus E (GPa)	6.02	7.9	8.64	9.07	3.23	4.18
Confining pressure σ_3 (MPa)	10.00	20.00	10.00	20.00	10.00	20.00
Pore pressure (top) (MPa)	7.00	7.00	7.00	7.00	7.00	7.00
Pore pressure (bottom) (MPa)	1.00	1.00	1.00	1.00	1.00	1.00
Osmotic pressure difference (MPa)	5.36~5.83	5.32~6.03	5.89~5.94	5.80~5.99	5.70	5.91~5.98
Peak stress σ_{1t} (MPa)	36.05	71.23	25.25	59.29	13.67	55.76
Peak strain	0.0212	0.0117	0.0137	0.0083	0.0038	0.0118
Permeability (Darzy)	1.55~1.75	0.94~1.21	4.19~6.92	3.72~5.26	8.30	6.83~7.30

(4) According to the data in Table 6, the seepage coefficient of cracked rock filled with gypsum mortar is in an integer multiple proportional relation to the joint length and has no change with confining pressure. The seepage coefficient of cracked rock filled with cement mortar is in an integer multiple inverse

Table 2: Seepage test results of cracked sandstone filled with cement mortar.

Conditions and results	2-1	2-2	2-3	2-4	2-5	2-6
Sample size (mm)						
D	48.57	48.13	48.31	48.25	48.26	48.29
H	98.64	98.41	99.21	98.80	98.17	99.02
Crack length (%)	25	25	50	50	75	75
Density ρ ($g\,cm^{-3}$)	2.34	2.32	2.31	2.32	2.30	2.31
Elastic modulus E (GPa)	6.94	8.39	6.09	8.92	6.53	9.02
Confining pressure σ_3 (MPa)	10.00	20.00	10.00	20.00	10.00	20.00
Pore pressure (top) (MPa)	7.00	7.00	7.00	7.00	7.00	7.00
Pore pressure (bottom) (MPa)	1.00	1.00	1.00	1.00	1.00	1.00
Osmotic pressure difference (MPa)	5.38~5.93	5.87~5.93	5.76~5.83	5.80~5.92	5.76~5.87	5.93~6.05
Peak stress σ_{1t} (MPa)	43.99	71.19	40.01	70.62	32.80	64.88
Peak strain	0.0081	0.0098	0.0067	0.0090	0.0054	0.0097
Permeability (Darzy)	7.94~8.67	3.51~3.64	8.35~9.84	4.72~4.90	11.62~11.85	5.85~6.06

Table 3: Seepage test results of intact sandstone.

Sample	Size (mm)	Density ρ ($g\,cm^{-3}$)	Elastic modulus E (GPa)	Confining pressure σ_3 (MPa)	Pore pressure (top) (MPa)	Pore pressure (bottom) (MPa)	Osmotic pressure difference (MPa)	Peak stress σ_{1t} (MPa)	Peak strain	Permeability (darzy)
0-1										
D	49.00	2.24	8.64	10.00	7.00	1.00	5.96~6.15	75.09	0.0101	1.35~1.7739
H	100.02									
0-2										
D	48.00	2.24	8.87	20.00	7.00	1.00	5.61~5.94	89.32	0.0128	0.63~0.94
H	99.55									

*1Darcy = $9.869 \times 10^{-9}cm^2$; *$\sigma_{1t} = \sigma_1 - \sigma_3$.

Table 4: Peak stress ratio of the filled cracked rocks.

Sample	$\sigma_{0-2}/\sigma_{0-1}$	$\sigma_{1-2}/\sigma_{1-1}$	$\sigma_{1-4}/\sigma_{1-3}$	$\sigma_{1-6}/\sigma_{1-5}$	$\sigma_{2-2}/\sigma_{2-1}$	$\sigma_{2-4}/\sigma_{2-3}$	$\sigma_{2-6}/\sigma_{2-5}$
Confining pressure ratio	2	2	2	2	2	2	2
Peak stress ratio	1.19	1.98	2.35	4.08	1.62	1.77	1.98

Table 5: Strength difference of the filled cracked rocks.

σ_3 = 10MPa	$\sigma_{1-1}-\sigma_{1-3}$	$\sigma_{1-1}-\sigma_{1-5}$	$\sigma_{2-1}-\sigma_{2-3}$	$\sigma_{2-1}-\sigma_{2-5}$
$\Delta\sigma_{1t}$	10.80 MPa	22.38 MPa	3.98 MPa	11.19 MPa
σ_3 = 20MPa	$\sigma_{1-2}-\sigma_{1-4}$	$\sigma_{1-2}-\sigma_{1-6}$	$\sigma_{2-2}-\sigma_{2-4}$	$\sigma_{2-2}-\sigma_{2-6}$
$\Delta\sigma_{1t}$	11.94 MPa	15.47 MPa	0.57 MPa	6.31 MPa

proportion relation to confining pressure, and its change value is much larger than that caused by crack length increase.

3.2. Discussion. In the rock triaxial seepage compression experiment, the opening of original cracks, the generating of new cracks, and the increase of pore space in rock make the pore pressure decrease and the effective stress increase, especially the effective confining pressure increase, which leads to an increase in rock strength. This is the dilatancy hardening [34]. In this paper, since the gypsum mortar in the filling crack dissolves and loses gelation in water, under the hydrodynamic force, the particles in the filling are washed and moved, and the particles enter the newly added pores, hindering the flow of pore water. This is not conducive to the reduction of pore pressure so that the strength changes of this kind filled cracked rock caused by the increase of effective confining pressure is not sensitive. The cracked rock filled with cement mortar is different. Cement is a hydraulic material, and it continues to exert its gelation effect in water so that the filling particles are not easily lost. And this

Table 6: Permeability of the filled cracked rocks.

Rock	1-1	1-3	1-5	2-1	2-3	2-5
Crack length (%)	25	50	75	25	50	75
σ_3 (MPa)	10	10	10	10	10	10
Permeability (Darzy)	1.55~1.75	4.19~6.92	8.30	7.94~8.67	8.35~9.84	11.62~11.85
Rock	1-2	1-4	1-6	2-2	2-4	2-6
σ_3 (MPa)	20	20	20	20	20	20
Crack length (%)	25	50	75	25	50	75
Permeability (Darzy)	0.94~1.21	3.72~5.26	6.83~7.30	3.51~3.64	4.72~4.90	5.85~6.06

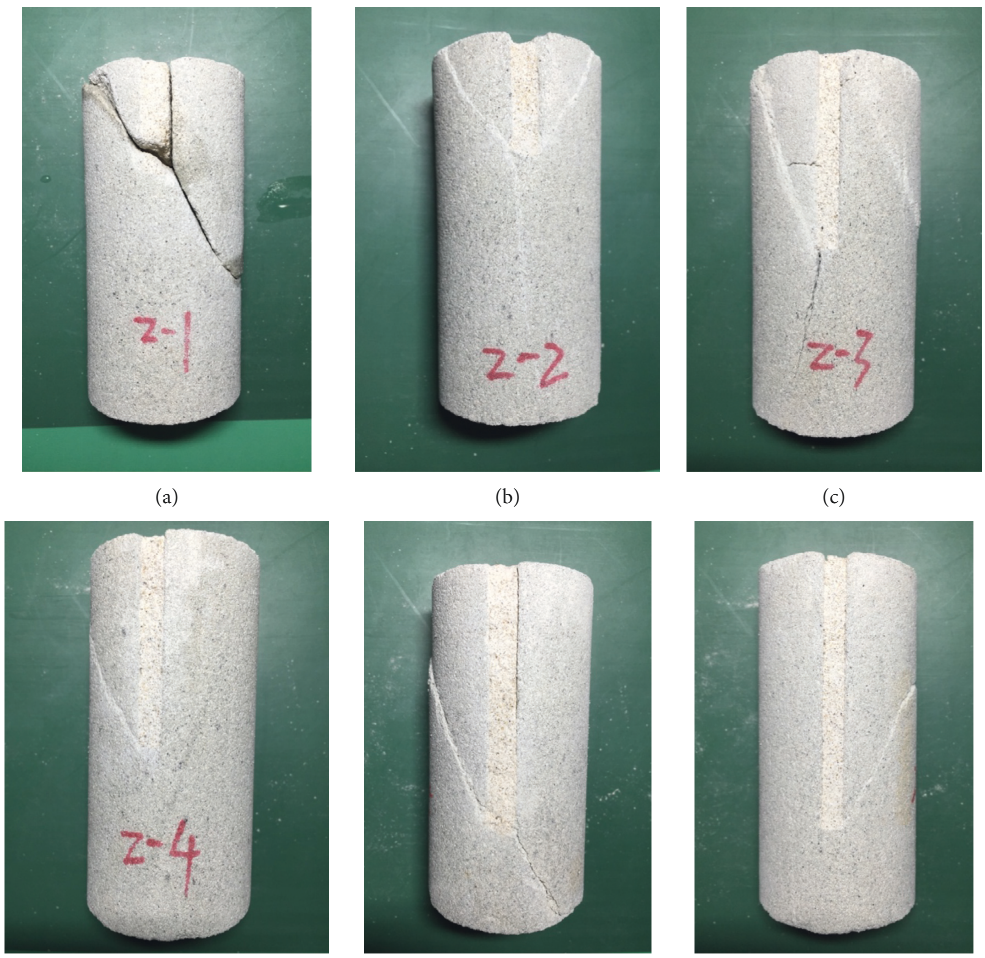

(a) (b) (c) (d) (e) (f)

Figure 8: Destruction pictures of cracked sandstone filled with cement mortar. (a) 2-1. (b) 2-2. (c) 2-3. (d) 2-4. (e) 2-5. (f) 2-6.

cracked rock filled with cement mortar has obvious failure crack and high continuity (as shown in Figure 8), which is favorable for the reduction of pore pressure, so it is significantly affected by the effective confining pressure.

Rocks are composed of mineral particles or grains, which are inhomogeneous and anisotropic at millimeter scale and have different scales of weak plane. In this test, with the increase of confining pressure, the peak stress growth rate of the filled cracked rock is significantly higher than that of the intact rock. Friction works when the rock is defective, and the friction between the end and the metal head is transmitted to the sample by the mineral particles to affect the strength. Thus the strength deviation of the sample is related to the internal crack. This shows that the end friction effect can have a significant impact and cause the strength of the filled cracked rock to be high. The increase of the confining pressure or the normal stress increases the bearing capacity of the defects, and the difference from the intact material will gradually decrease.

The effect of confining pressure on the permeability of the filled cracked rock is related to the sample internal

(a) (b)

Figure 9: Complete sandstone destruction pictures. (a) 0-1. (b) 0-2.

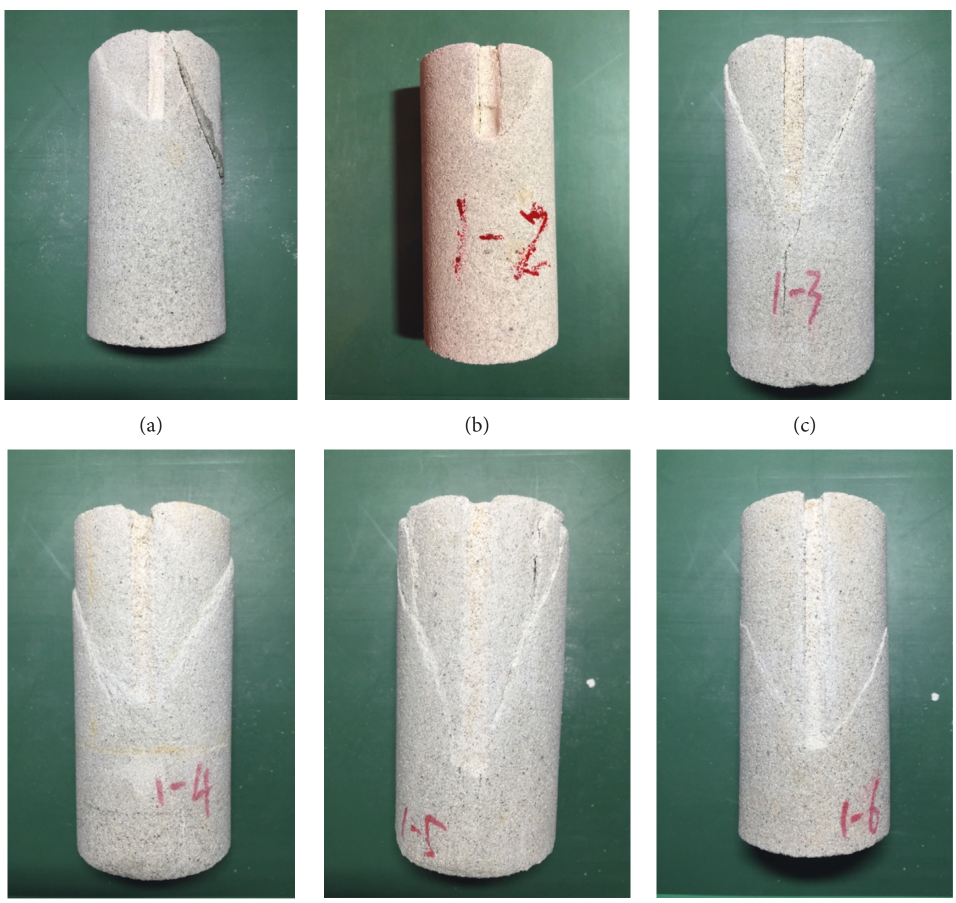

(a) (b) (c)

(d) (e) (f)

Figure 10: Destruction pictures of cracked sandstone filled with gypsum mortar. (a) 1-1. (b) 1-2. (c) 1-3. (d) 1-4. (e) 1-5. (f) 1-6.

structure. The framework grains, cracks, and fillings in the filled cracked sandstone are compressed so that the samples show compression deformation. With the increase of confining pressure, the sandstone volume deformation increases gradually, which leads to the increase of the crack closure and the decrease of the permeability channels and consequently leads to the gradual decrease in the permeability.

The equation of the hydraulic conductivity coefficient of the parallel crack surface proposed by Schrauf and Evans [35] is

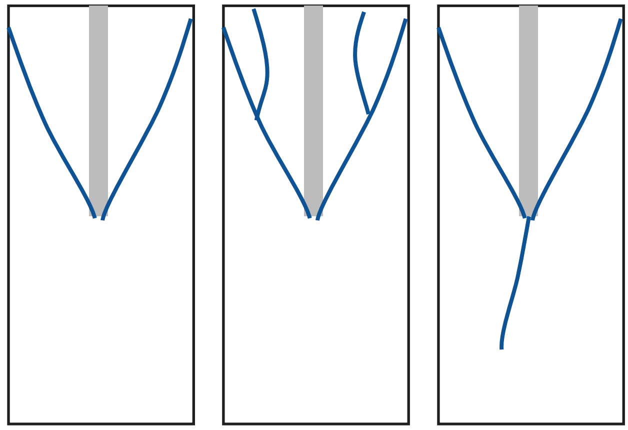

Figure 11: Macrofailure mode sketch. (a) Type 1. (b) Type 2. (c) Type 3.

$$K_f = \frac{kge^2}{12\mu c}, \quad (2)$$

where k is the crack continuity index, e is the crack width, and c and d are the relative roughness coefficients. In the seepage test of cracked rock filled with cement mortar, considering that the cement has gelation in water and the filling is not lost, the permeability of rock with different joint lengths is less affected by the crack continuity index. However, it is obviously affected by the compression of the confining pressure, the crack width becomes smaller, and the permeability affected by the width is a square change. Therefore, due to the influence of increased confining pressure, the permeability of cement mortar filled cracked rock is greatly reduced. In the fractured rock filled with gypsum mortar, since that it is not sensitive to the confining pressure and the filling particles are easily washed away, the permeability is more affected by the preset crack length. Moreover, the lost filling particles are easy to block the pore space in the rock, which makes the permeability of the fractured rock filled with gypsum mortar generally lower than that of the fractured rock filled with cement mortar.

3.3. Failure Mode. The complete sandstone rupture in the triaxial seepage test is characterized by significant shear failure (Figure 9). A shear slip occurs along the rupture surface, and the angle between the fracture surface and the maximum compressive stress direction is less than 45°. However, even under different confining pressures, the cracks of intact rocks are similar, and the failure modes are consistent, indicating that the failure characteristics of intact rocks are not affected by water pressure and confining pressure.

As shown in Figures 10 and 8, with the increase of preset crack length, the shear crack length that sprout from the top also increases, which is directly proportional to it. Different from the intact rock, the failure of filled cracked rock in the seepage test is influenced by confining pressure and water pressure. Compared with those under high confining pressure, the filled cracked rocks show more secondary cracks under lower pressure. However, due to the filler and their different physical properties under water pressure, the cracked rock failure characteristics are also different. In the cracked sandstone filled with gypsum mortar, small tensile cracks at the end of the rocks in Figure 10 can be observed, as the filling material migrates under the hydrodynamic force, and the water carries gypsum mortar into the open crack, which causes further deformation and damage. As shown in Figure 8, in the cracked sandstone filled with cement mortar, the development of microcracks is not obvious, but a large tensile crack sprouted along the end of the crack.

Figure 11 is a sketch of the macroscopic failure mode of filled fractured sandstone. According to the different failure formation mechanism, the secondary cracks of rocks under the seepage stress can be divided into 3 categories:

(1) Type I is a tensile-shear mixed crack that initiates from the tip of the preset crack to the end of it.
(2) Type II is a distal tensile crack caused by the migration of the filling.
(3) Type III is a tensile crack that develops from the region of tensile stress concentration near the tip of the preset crack and develops in the direction of the hydrodynamic force direction.

The percolation failure modes of single crack sandstones with different fillings can be classified into 2 types:

(1) In the cracked sandstone filled with gypsum mortar (Types 1 and 2), the shear cracks generated from the tip of the crack and connected to the upper end of the rock to form a “cone” structure that no longer bears load, leading to instability and failure, accompanied by a small number of distal tensile cracks.
(2) In the cracked sandstone filled with cement mortar (Type 3), the tensile-shear mixing crack propagates from the preset crack tip to the entire rock, resulting in the overall instability of the rock.

4. Conclusion

In order to understand the strength, deformation, permeability, and failure law of filled cracked rock, the triaxial compression seepage experiments of cracked sandstones filled with gypsum mortar and the ones filled with cement mortar are carried out, under the confining pressure of 10 MPa and 20 MPa and the water pressure of 7 MPa.

According to the laboratory seepage tests, the following conclusions are obtained. (1) The permeability coefficient peak value of the filled cracked rocks appears before the stress peak. (2) The peak stress of intact rock and filled fractured rock increases with the increase of confining pressure. At the same confining pressure growth rate, the stress growth rate of the fractured rock is significantly higher than that of the intact rock, and the stress growth rate of the fractured rock increases with the increase of the crack length. (3) The strength and permeability coefficient of cracked rock filled with cement mortar are more sensitive to the change of confining pressure because this filler can still work synergistically with the original rock in the water, so it is obviously affected by confining pressure confinement effect. However, under the same condition, the ones of cracked rock filled with gypsum mortar are stable. The permeability coefficient of cracked rock filled with gypsum mortar is sensitive to the change of crack length because of the fluidity of gypsum mortar; the preset cracks become the dominant one to expand the flow path and significantly affect the permeability change. (4) The seepage failure modes of filled cracked rocks can be divided into 2 categories. One is that the shear cracks initiated from the fracture tip and extended to the end lead to "cone" structure and failure, and the other is the tensile-shear mixed cracks initiated from the preset crack tip and extended to the whole rock leading to the overall instability.

Data Availability

Demand data used to support the findings of this study are available from the first author upon request.

Conflicts of Interest

The authors declare that there are no conflicts of interest regarding the publication of this paper.

Acknowledgments

This study was supported by the National Natural Science Funds (41831278 and 51579081) of China and the Guangdong Province Water Resource Science and Technology Innovation Program (2017–30) of China.

References

[1] Y. Xing, C. Zhang, and J. Wang, "Analysis and regularity of China's coal mine water inrush accident in 2007~2014," *Coal Technology*, vol. 35, no. 7, pp. 186–188, 2016.

[2] B. Shi and Z. Hou, "Mechanical analysis of fault activation water inrush in over burden rock and its application," *Rock and Soil Mechanics*, vol. 32, no. 10, pp. 3053–3057, 2011.

[3] S. Cai and F. Li, "The research on the destroy law of seepage in crack-rockmasses," *Electric Power Survey*, vol. 26, no. 2, pp. 4–7, 2000.

[4] Y. W. Tsang and P. A. Witherspoon, "Hydromechanical behavior of a deformable rock fracture subject to normal stress," *Journal of Geophysical Research: Solid Earth*, vol. 86, no. B10, pp. 9287–9298, 1981.

[5] Z. Q. Wei, P. Egger, and F. Descoeudres, "Permeability predictions for jointed rock masses," *International Journal of Rock Mechanics and Mining Sciences & Geomechanics Abstracts*, vol. 32, no. 3, pp. 251–261, 1995.

[6] P. Dijk, B. Berkowitz, and P. Bendel, "Investigation of flow in water-saturated rock fractures using nuclear magnetic resonance imaging (NMRI)," *Water Resources Research*, vol. 35, no. 2, pp. 347–360, 1999.

[7] N. Coli, G. Pranzini, A. Alfi, and V. Boerio, "Evaluation of rock-mass permeability tensor and prediction of tunnel inflows by means of geostructural surveys and finite element seepage analysis," *Engineering Geology*, vol. 101, no. 3-4, pp. 174–184, 2008.

[8] A. Baghbanan and L. Jing, "Hydraulic properties of fractured rock masses with correlated fracture length and aperture," *International Journal of Rock Mechanics and Mining Sciences*, vol. 44, no. 5, pp. 704–719, 2007.

[9] A. Baghbanan and L. Jing, "Stress effects on permeability in a fractured rock mass with correlated fracture length and aperture," *International Journal of Rock Mechanics and Mining Sciences*, vol. 45, no. 8, pp. 1320–1334, 2008.

[10] J. Liu, Y. U. Zhenmin, R. Wang, and L. Jianlin, "Research on seepage law of splitting sandstone with non-fillers under multiple factors," *Journal of Hydraulic Engineering*, vol. 47, no. 1, pp. 54–63, 2016.

[11] A. K. M. B. Alam, M. Niioka, Y. Fujii, D. Fukuda, and J.-i. Kodama, "Effects of confining pressure on the permeability of three rock types under compression," *International Journal of Rock Mechanics and Mining Sciences*, vol. 65, no. 1, pp. 49–61, 2014.

[12] K.-B. Min, J. Rutqvist, C.-F. Tsang, and L. Jing, "Stress-dependent permeability of fractured rock masses: a numerical study," *International Journal of Rock Mechanics and Mining Sciences*, vol. 41, no. 7, pp. 1191–1210, 2004.

[13] M. N. Bidgoli and L. Jing, "Water pressure effects on strength and deformability of fractured rocks under low confining pressures," *Rock Mechanics & Rock Engineering*, vol. 48, no. 3, pp. 971–985, 2015.

[14] R. Zhang, Z. Jiang, Q. Sun, and S. Zhu, "The relationship between the deformation mechanism and permeability on brittle rock," *Natural Hazards*, vol. 66, no. 2, pp. 1179–1187, 2013.

[15] L. Wang, J.-f. Liu, J.-l. Pei, H.-n. Xu, and Y. Bian, "Mechanical and permeability characteristics of rock under hydro-mechanical coupling conditions," *Environmental Earth Sciences*, vol. 73, no. 10, pp. 5987–5996, 2015.

[16] P. E. C. D. Toledo, M. H. D. Freitas, and CGcol, "Laboratory testing and parameters controlling the shear strength of filled rock joints," *Geotechnique*, vol. 43, no. 1, pp. 1–19, 1993.

[17] M. C. R. Davies, O. Hamza, B. W. Lumsden, and C. Harris, "Laboratory measurement of the shear strength of ice-filled rock joints," *Annals of Glaciology*, vol. 31, no. 1, pp. 463–467, 2000.

[18] B. Indraratna, M. Jayanathan, and E. T. Brown, "Shear strength model for overconsolidated clay-infilled idealised rock joints," *Géotechnique*, vol. 58, no. 1, pp. 55–65, 2008.

[19] J. C. Li, W. Wu, H. B. Li, J. B. Zhu, and J. Zhao, "A thin-layer interface model for wave propagation through filled rock joints," *Journal of Applied Geophysics*, vol. 91, no. 4, pp. 31–38, 2013.

[20] G. P. Wealthall, A. Steele, J. P. Bloomfield, R. H. Moss, and D. N. Lerner, "Sediment filled fractures in the Permo-Triassic sandstones of the Cheshire Basin: observations and implications for pollutant transport," *Journal of Contaminant Hydrology*, vol. 50, no. 1-2, pp. 41–51, 2001.

[21] Q. Chen and W. Kinzelbach, "An NMR study of single and two phase flow in fault gouge filled fractures," *Journal of Hydrology*, vol. 259, no. 1–4, pp. 236–245, 2002.

[22] J. E. Olson, S. E. Laubach, and R. H. Lander, "Natural fracture characterization in tight gas sandstones: integrating mechanics and diagenesis," *Aapg Bulletin*, vol. 93, no. 11, pp. 1535–1549, 2009.

[23] G. Wang, W. Liu, and Y. Tao, "Experimental study of permeability in fractured sandstone with sediment particles," *Mechanics in Engineering*, vol. 32, no. 5, pp. 14–17, 2010.

[24] J. Thörn, L. O. Ericsson, and Å. Fransson, "Hydraulic and hydromechanical laboratory testing of large crystalline rock cores," *Rock Mechanics and Rock Engineering*, vol. 48, no. 1, pp. 61–73, 2015.

[25] T. Ono, H. Yoshida, and R. Metcalfe, "Use of fracture filling mineral assemblages for characterizing water-rock interactions during exhumation of an accretionary complex: an example from the Shimanto Belt, southern Kyushu Japan," *Journal of Structural Geology*, vol. 87, pp. 81–94, 2016.

[26] J. L. Kavanagh and M. J. Pavier, "Rock interface strength influences fluid-filled fracture propagation pathways in the crust," *Journal of Structural Geology*, vol. 63, pp. 68–75, 2014.

[27] J. Liu, J. Li, J. Hu, C. Jian, and Z. Zong-Yong, "Comparative analysis of multiple factors affecting seepage flow of splitting sandstone with fillers or non-fillers," *Rock and Soil Mechanics*, vol. 35, no. 8, pp. 2163–2170, 2014.

[28] L. Zhang, J. Chen, and J. Han, "Effect of microstructure on seepage-stress characteristics of half-filled fracture," *Safety and Environmental Engineering*, vol. 22, no. 4, pp. 160–163, 2015.

[29] J. Chen and J. Zhang, "Influence of mechanical responses of fillings on fracture seepage," *Rock and Soil Mechanics*, vol. 27, no. 4, pp. 577–580, 2006.

[30] J. Chen, L. Zhang, and J. Fan, "Seepage-stress characteristics of brittle-plastic filled fracture," *Journal of Mining & Safety Engineering*, vol. 33, no. 6, pp. 1103–1109, 2016.

[31] X. Liu, A. Liu, and X. Li, "Experimental study of permeability of rock-like material with filling fractures under high confining pressure," *Chinese Journal of Rock Mechanics and Engineering*, vol. 31, no. 7, pp. 1390–1398, 2012.

[32] H. Xie, F. Gao, J. Yang et al., "Quantitative definition and investigation of deep mining," *Journal of China Coal Society*, vol. 40, no. 1, pp. 1–10, 2015.

[33] M. He, H. Xie, S. Peng et al., "Study on rock mechanics in deep mining engineering," *Chinese Journal of Rock Mechanics and Engineering*, vol. 24, no. 16, pp. 2803–2813, 2005.

[34] Y. Chen, T. Huang, and E. Liu, *Rock Physics*, Press of USTC, Hefei, Anhui, China, 2009.

[35] T. W. Schrauf and D. D. Evans, "Laboratory studies of gas flow through a single natural fracture," *Water Resources Research*, vol. 22, no. 7, pp. 1038–1050, 1986.